RECIPROCATING PUMP VALVE DESIGN

by

Gerhard Vetter

Professor and Head of the Department for Apparatus and Chemical Machinery

and

Erwin Thiel

Research Engineer

Universität Erlangen-Nürnberg

Erlangen, West Germany

and

Ulrich Störk

Service Engineer

Lewa Herbert Ott GmbH Company

Lewa Leonberg, West Germany

Gerhard Vetter obtained his Dipl.-Ing.-degree in Mechanical Engineering at Technische Universität Karlsruhe, West Germany. After some years as Research Engineer in turbomachinery and thermal power engineering at the same university, he joined Lewa Herbert Ott GmbH and Company, as head of the Research and Development Department. He became Chief Engineer and, in 1970, Technical Managing Director. In 1981, he accepted a professorship for Apparatus and Chemical Machinery at Universität Erlangen-Nürnberg, West Germany, and remains Lewa's Research and Development Consultant.

Professor Vetter has dedicated more than 25 years to research, development and design of pumps and metering equipment. He has been one of the pioneers in diaphram pump development, especially their application for dangerous and abrasive liquids, high pressures, high power, safety systems, metering accuracy and reliability. Many papers, patents and contributions to text books—some dealing with basics like cavitation, fatigue, pulsation, vibrations, and metering accuracy—have established his reputation as a pump specialist.

Erwin Thiel obtained his Dipl.-Ing.-degree in Mechanical Engineering at Technische Universität Stuttgart, West Germany. After some years as Research Engineer at the same university, he joined Professor Vetter's Institute at Erlangen University in 1983. There he is responsible for various research projects, especially hydrodynamics and kinematics of pump valves. He is an expert on dynamic measurement and numerical computation for dynamic processes.

Ulrich Störk obtained his Dipl.-Ing.-degree in Mechanical Engineering at Technische Universität Stuttgart, West Germany. After two years with Lewa, in Leonberg as a Research Engineer, he joined Professor Vetter's Institute at Erlangen University in 1983. He performed a scientific investigation on valve wear which was finalized by a doctoral dissertation. In 1988, Dr. Störk returned to Lewa, in Leonberg as Chief Service Engineer.

ABSTRACT

The working mechanism and life expectancy of automatic pump check valves, which are important for the operational safety of oscillating displacement pumps, are closely examined. A calculation process for the determination of the valve kinematic and pressure losses is discussed, which is based on hydrodynamic coefficients. These coefficients are dependent on the Reynolds number. It also is based on the force equilibrium exerted on the active valve body.

It is shown that a numerical calculation can correctly determine closing delay, closing speed and valve pressure losses for Newtonian liquids.

A design strategy is shown for the prognosis of life expectancy of automatic check valves. It is based on the tribometric simulation in a tamping tribometer. Field tests have shown that the tribometric simulation is close to reality. However, the tribosystem must necessarily be operated in its stable range to eliminate radial erosion. In addition to the relative hardness of the construction material or to the abrasive particles, the SAR-Number, which should be smaller than 90-100, is an important indicator.

The investigations are a substantial contribution to the design improvement of automatic pump check valves.

INTRODUCTION

The flowrate of oscillating positive displacement pumps (Figure 1) for a given stroke volume $A_K h_K$ is linearly proportional to the stroke frequency n [1].

$$\dot{m} = \rho A_K \cdot h_K \cdot n \cdot \eta_E \cdot \eta_G \qquad (1)$$

The geometric displacement of the stroke volume is reduced by the volumetric efficiency.

$$\eta_V = \eta_E \cdot \eta_G \qquad (2)$$

The elasticity factor η_E represents the influence of the compressibility of the fluid and the elasticity of the working chamber; interior and exterior leakages will be considered as the quality or slip factor η_G.
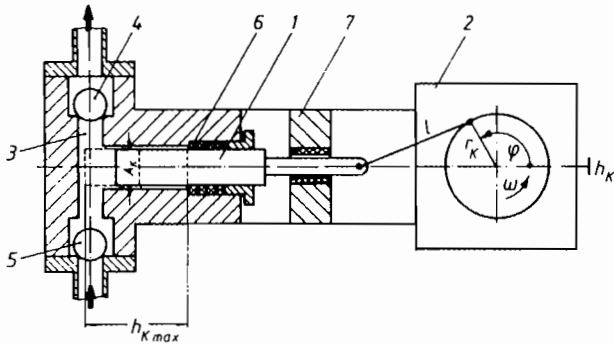

Figure 1. Schematic View of a Plunger Pump with Automatic Check Valves. 1) plunger, 2) drive elements, 3) working chambers, 4) discharge valves, 5) suction valves, 6) seals, 7) cross head.

To optimize performance, it is desirable to operate oscillating metering pumps at high frequencies. One of the most important factors limiting the stroke frequency is the automatic check valve. The check valves should control the intermittent flow (opening and closing) with a minimum of pressure loss and wear. Therefore, the kinematics of the valve bodies (cone, ball plate, disc) is of great importance. It is determined by the governing power equilibrium.

In the valve opening phase (Figure 2), especially on the suction side, the pressure loss which determines $NPSH_r$ is of special importance. The smaller the $NPSH_r$, the less critical the layout on the suction side of the pump. The valve closing delay has to be kept short, as the resulting interior leakage/slip of the fluid
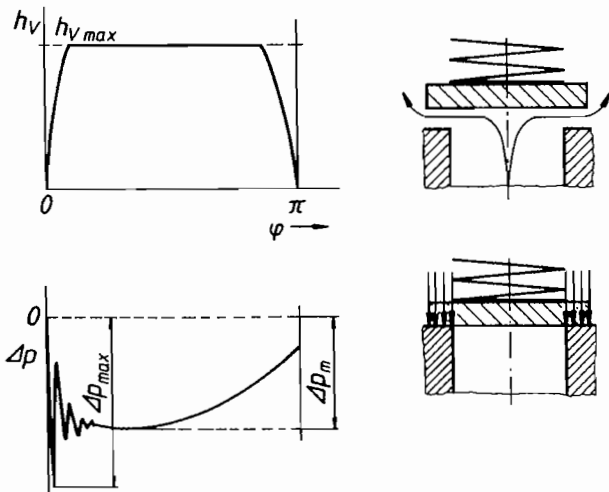

Figure 2. Kinematic and Pressure Loss. h_v lift of valve body, Δp pressure loss, φ crank angle.

leads to a loss of effective displacement volume and therefore a lesser flowrate. In Equation (1), the quality factor η_G is accordingly reduced.

For most of the common straight connecting rod crank drives, the resulting losses can be estimated from the calculated loss in stroke volume (Figure 3). The closing delay of the check valve causes an additional change in the real displacement characteristic in the direction of higher pressure shocks, which affects the pump pulsation unfavorably.

With closed valves, the stress on the sealing surfaces plays an important role. When the valve body strikes the valve seat, a specific closing energy is released with

$$E_s = \frac{m \cdot \dot{h}_v^2}{2A_{VF}} \qquad (3)$$

Stress on the construction material is the limiting factor.

During the resting phase of the closed valves, the seat is exposed according to the differential pressure to a pulsating and generally higher compression, which, especially with abrasive slurries, significantly determines the wear characteristics [2].

Progress in the calculation of the hydrodynamics and kinematics of automatic check valves is discussed herein. Construction of check valves for the metering of abrasive fluids will also be addressed.

HYDRODYNAMICS AND KINEMATICS

Mathematic Model of Check Valve Kinematics

The customary plunger movement is usually partially harmonic or corresponds to the movement of common straight connecting rod crank drives (Figure 1). For $\lambda_K = r_K / l$

$$h_K = r_K \cdot (1 - \cos\varphi - \frac{\lambda_K}{2} \cdot \sin^2\varphi) \qquad (4)$$

$$v_K = r_K \cdot \omega \cdot (\sin\varphi - \frac{\lambda_K}{2} \cdot \sin2\varphi) \qquad (5)$$

(λ_K connection rod relation, r_K crank radius, l length of connecting rod, h_K Stroke length of plunger, φ crank angle, v_K plunger velocity, ω angular velocity).

The corresponding relationships for gears with harmonic kinematics are obtained for $\lambda_K = 0$.

For a given plunger movement (h_k, v_K) the resulting valve kinematic (h_v) and pressure in the pumping chamber are schematically presented in Figure 3. The elasticity of fluid and pumping chamber, as well as the closing delay of the check valve, result in a significant opening angle φ_0 and closing angle φ_s (closing delay $\Delta\varphi_s$). Also evident is the resulting phase rise of the displacement velocity Δv_K. The moving valve body can reach its limit (h_{Vmax}).

Every delay in the closing of the check valves results in filling fluid volume losses and fluid depending metering errors in positive displacement pumps. The relation of the plunger stroke with closed valve h_K (φ_s) to the complete plunger stroke $h_{K,max}$, results in first approximation in the effective degree of quality loss (Figure 4).

$$\Delta\eta_{GS} = \frac{h_K(\varphi_S)}{h_{K,max}} \qquad (6)$$

If both the suction and discharge check valves of a pump have the same closing delay, then the value of Figure 4 doubles. The degree of quality η_G in Equation (1) is the result of fluid loss through the delay of closing (slip) of both check valves and leakages in the seals of plunger and pump valves.
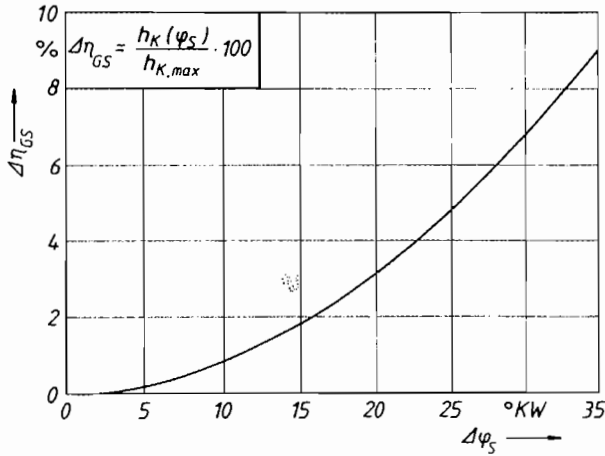
Figure 3. *Plunger and Valve Kinematic and Pumping Chamber Pressure (schematic) DS discharge stroke, SS suction stroke, DV discharge valve, SV suction valve.*

$$\eta_G = 1 - (\Delta\eta_{GSs} + \Delta\eta_{GSd}) - \sum \Delta\eta_{GI} \qquad (7)$$

The valve "slip" is only a part of the generally small leakages. The degree of quality in correctly designed oscillating positive displacement pumps is generally close to one.
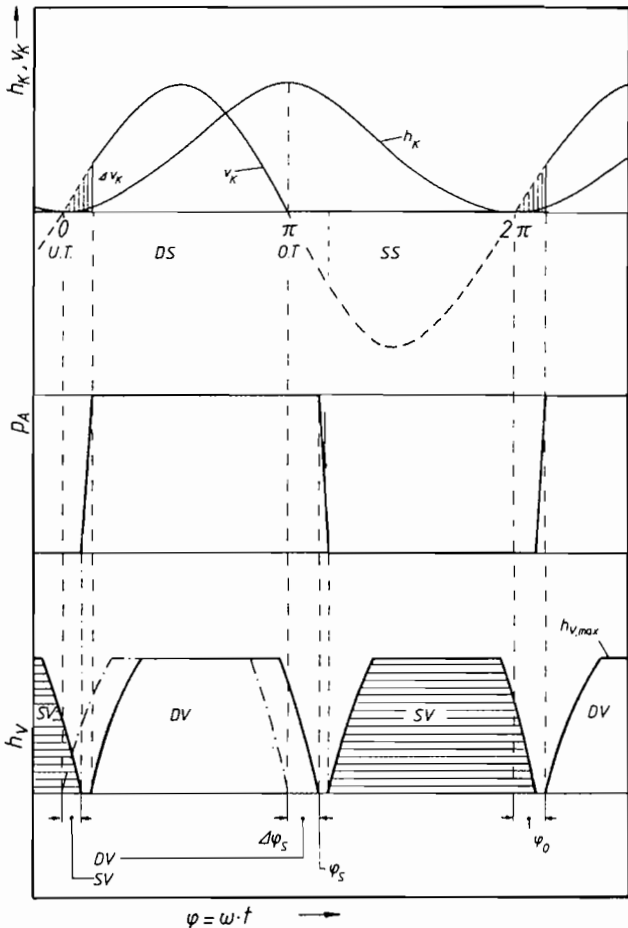

Figure 4. *Reduction of Quality (Slip) Factor through Check Valve Closing Delay.*

EQUILIBRIUM OF FORCES

The check valve kinematics is the result of the equilibrium of forces [3] on the valve body (Figure 5).

$$F_{St} + F_G + F_F + F_D + F_R + F_a + F_V + F_{Ad} = 0 \qquad (8)$$

The effective forces in detail:
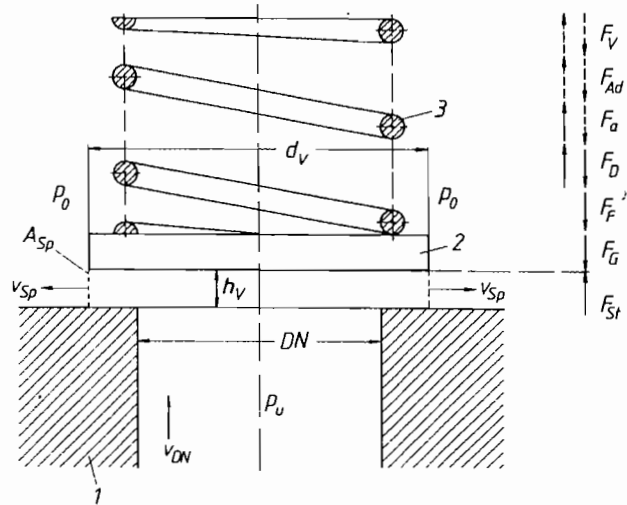
Force of Fluid Stream F_{St}

Figure 5. *Equilibrium of Forces and Nomenclature as Shown for a Plate Valve. 1) valve seat, 2) valve plate (body), 3) valve spring.*

If a fluid is forced through a valve, a differential pressure (p_u p_o) is established in relation to a control level at some distance from the aperture. This force is

$$F_{St} = 2\pi \int r \left(p_u^*(r) - p_o^*(r) \right) \, dr \qquad (9)$$

when p_u^* and p_o^* designate the pressure levels that directly affect the moving valve body. The pressure distribution is not constant, at least on the upstream side, above the radius of the valve body r_v. The resulting force F_{St} is, therefore, best established [3] with an empirically measured force coefficient Ψ that depends on the Reynolds number.

$$F_{St} = \psi \cdot (p_u - p_o) \cdot A_v \qquad (10)$$

where the area A_v is the cross section of the valve body which has an outer diameter of d_v.

Gravitational Force F_G

$$F_G = g \cdot (\rho_{Mat} - \rho_{Fl}) \cdot V_{Mat} \qquad (11)$$

(g gravitational acceleration, ρ_{Mat} density of valve body, ρ_{Fl} density of fluid, V_{Mat} volume of valve body).

Force of Spring F_F

$$F_F = F_{F0} + k_F \cdot h_v \qquad (12)$$

(F_{F0} spring tension, k_F spring constant, h_v displacement of valve body).

Force of Damping/Friction F_O

For fluid friction, an equation proportional to the speed has been selected.

$$F_D = \vartheta \cdot \dot{h}_v \qquad (13)$$

(ϑ Dampening factor, experimentally determined, depends on Reynolds number, $\dot{h}_v$ velocity of valve body).

Force of Mechanical Friction F_R

$$F_R = \mu \cdot F_N \qquad (14)$$

With a known normal force F_N that is caused within the valve guide, a friction force results with a friction coefficient μ. For plate valves without guide (Figure 5) $F_R = 0$.

Force of Inertia F_a

$$F_a = \left(m_V + \frac{1}{3} \cdot m_F \right) \cdot \ddot{h}_V = m \cdot \ddot{h}_V \qquad (15)$$

Where m_V is the mass of the valve body, and m_F the mass of the spring, which contributes a $\frac{1}{3}$ share [3] ($\ddot{h}_V$ is acceleration of the valve body).

Immediately at the opening of the check valve, a negative spike of inertia is formed; during the valve movement F_a becomes positive and disappears when the valve body is at rest (upper resting position $\ddot{h}_V = 0$).

Force of Displacement F_V

This force is caused when the valve body approaches a limit (upper limit or valve seat). The fluid then has to be displaced radially, which requires noticeable forces for higher viscosities.

Force of Adhesion F_{Ad}

The dislodging of the pressed on valve body causes (as does the force of displacement) pressure peaks for higher viscosities (opening of valves with wide seat). Forces of adhesion can also appear at the upper limit of the valve. For most practical applications F_D, F_R, F_V and F_{Ad} can be neglected as insignificant. The limitations of this omission will be shown later.

CONTINUITY, PRESSURE LOSS IN APERTURE

The displaced volume in a given time $A_K \times v_K$ equals the sum of the displaced flow volume through the valve aperture $\dot{V}_{Sp}$, the volume displaced by the valve body $A_V \times h_V$ and the elasticity volume (fluid and working chamber) $\dot{V}_{dp}$

$$A_K \cdot v_K = \dot{V}_{Sp} + A_v \cdot \dot{h}_V + \dot{V}_{dp} \qquad (16)$$

The resulting aperture flow $\dot{V}_{Sp}$ can be derived directly from Figure 5 with the discharge flow equations

$$\dot{V}_{Sp} = A_{Sp} \cdot v_{Sp} = l_{Sp} \cdot h_V \cdot \sqrt{\frac{2 \cdot (p_u - p_o)}{\zeta \cdot \rho \cdot \varepsilon}} \qquad (17)$$

$$v_{Sp} = \sqrt{\frac{2 \cdot (p_u - p_o)}{\zeta \cdot \rho \cdot \varepsilon}} \qquad (18)$$

where

ζ	resistance coefficient depends on Reynolds number
$A_{Sp} = l_{Sp} \cdot h_V$	aperture for plate valves
resp. $= l_{Sp} \cdot h_V \cdot f(\alpha)$	aperture area for cone valves
$\varepsilon \begin{cases} = 1; \ p_u - p_o > 0 \\ = -1; \ p_u - p_o < 0 \end{cases}$	
$l_{Sp} = d_{Vm} \cdot \pi$	length of aperture
α	angle of the valve closure area to the center axis of the valve
d_{Vm}	mean diameter of the seat

DIFFERENTIAL EQUATION OF THE VALVE MOVEMENT $h_{V(t)}$

The simplified equilibrium of forces with continuity and discharge equation yields the differential equation (non-linear of second order):

$$\frac{m\ddot{h}_V}{k_F} + h_V + \frac{F_G + F_{F0}}{k_F} - \frac{\varepsilon \cdot \psi \zeta \rho \cdot A_K^2 \cdot A_V \cdot v_K^2}{2 \cdot h_V^2 \cdot l_{Sp}^2 \cdot k_F} +$$

$$\frac{\varepsilon \cdot \psi \zeta \rho \cdot A_K \cdot A_V^2 \cdot v_K \cdot \dot{h}_V}{h_V^2 \cdot l_{Sp}^2 \cdot k_F} + \frac{\vartheta \cdot \dot{h}_V}{k_F} -$$

$$\frac{\varepsilon \cdot \psi \zeta \rho \cdot A_V^3 \cdot \dot{h}_V^2}{2 \cdot h_V^2 \cdot l_{Sp}^2 \cdot k_F} = 0 \qquad (19)$$

which is solved in approximation [4] numerically.

It should also be mentioned that $\dot{V}_{dp}$ in Equation (16) was omitted as negligible, however, in its stead the opening angle of the valve $\varphi_\ddot{O}$ that is derived from the volumetric efficiency η_W is entered in the calculation. If the influence of elasticity is omitted as insignificant, then $\varphi_\ddot{O}$ approximately equals the closing angle φ_S which has been determined in a prior calculation. Please refer to known methods for the calculation of the degree of elasticity η_E [5, 6].

The first usage of Equation (19) follows immediately after $\varphi_\ddot{O}$ Due to the omission (for example of F_{Ad}), the starting condition cannot be entered exactly. This, however, has little effect on either the maximum movement of the valve body, or on the closing angle φ_S.

INPUT DATA FOR THE CALCULATION PROGRAM

Valve

m	kg	: Mass of valve body and $\frac{1}{3}$ mass of spring
F_G	N	: Weight of valve body less buoyancy
F_{F0}	N	: Spring tension
k_F	N/m	: Spring constant
α		: Angle of valve closing area to horizontal (for example, cone angle)
d_V	m	: Outer diameter of valve body
d_{Vm}	m	: Mean diameter of closing area for the determination of flow area
h_{Vmax}	m	: Max. valve lift
$\varphi_\ddot{O}$		: Opening angle (degree of crank angle —from lower turning point (U.T.) for discharge valve), from uppoer point (O.T.) for suction valve

Pump

n	min−1	: Stroke frequency (rpm of pump)
r_K	m	: Crank radius
λ_K		: Connecting rod relation
d_K	m	: Plunger diameter

Fluid

η	Pas	: Dynamic fluid viscosity
ρ_{Fl}	kg/m³	: density of fluid

Calculation Program Control

$\Delta\varphi$	°	: Increment of calculation
φ_{End}	°	: End of calculation

Constants

For the calculation of ζ, ψ and ϑ that are dependent on the Reynolds number

EXPERIMENTAL DATA FOR CHECK VALVES ON PUMPS

Tests were performed using different valve constructions (Figure 6) for the determination of the coefficients of resistance and force, ζ and Ψ, which are dependent on the Reynolds number.
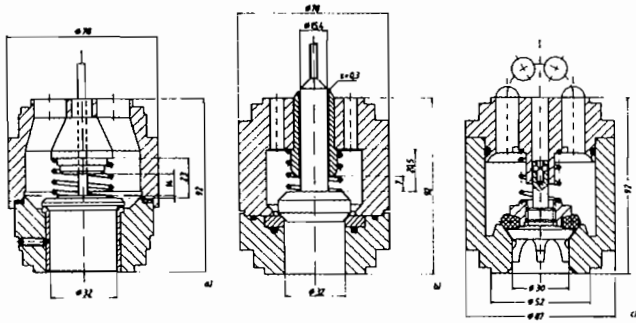

Figure 6(a-c). Pump Check Valves for Testing a) plate valve, b) cone valve with narrow seat, c) cone valve with broad seat.

The fluids used were water and water polyglycol mixtures of different viscosities.

$$\text{Resistance coefficient } \zeta = \frac{2 \cdot \Delta p}{v_{Sp}^2 \cdot \rho} \quad (20)$$

$$\psi = \frac{F_G + F_{F0} + k_F \cdot h_V}{\Delta p \cdot A_V} \quad (21)$$

$$\text{Reynolds number } Re_{Sp} = \frac{v_{Sp} \cdot d_h \cdot \rho}{\eta} \quad (22)$$
(aperture)

Symbols as previously noted in Fig. 5, plus the following:

v_{Sp}	Fluid velocity through valve aperture
$\Delta p = p_o - p_u$	Pressure differential as measured in a sufficient distance from the aperture
η	Dynamic viscosity of fluid
$d_h = 2 \cdot h_V$	Hydraulic diameter of aperture (or $d_h = 2 \cdot h_V \cdot \sin\alpha$ for cone valves)

Earlier examinations [7, 8] showed that under these flow conditions, statically determined values for ξ and Ψ also well represent dynamic pressure conditions. Both the resistance and force coefficients were determined dynamically directly on an operating pump (simplex $h_K = 45$ mm, $d_K = 70$ mm, $\lambda_K = 0.2$, n = 100-600 min^{-1}), as well as statically in a fluid circuit (multicylinder plunger pump with pulsation damper) with fixed flow volume. The test valve was operated with free movement and in predetermined adjustment of the valve body.

The ζ, Ψ values were entered under consideration of the aperture related Reynolds number.

Static and dynamic measurements generally coincide satisfactorily within the bounds of experimental error (Figure 7).

The ζ-Re-relationship with free floating valve body can be analytically represented in approximation:
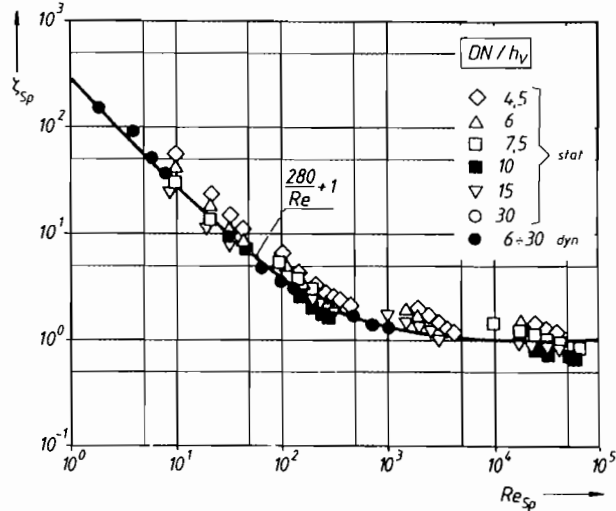
$$\zeta_{Sp} = \frac{A}{Re_{Sp}} + C \quad (23)$$

Figure 7. Resistance Coefficient ζ as Function of the Reynolds Number; Cone Valve with Narrow Seat 32mm ND.

(A and C are constants of the ζ-Re-function.)

For the plate valve with narrow seat (Figure 6(a)), for example, A = 200 and C = 2.0. With a wide movement of the valve body, however, the flow pattern does not remain uniform throughout. The pattern of the fluid flow changes. Re-dependent values are a function of the magnitude of valve movement.

This is less pronounced with cone shaped valves. With plate valves, the flow of the fluid changes from radial to conical with increasing movement (Figure 8) of the valve body. The influence of the magnitude of the movement of the valve body can be approximated as follows:

$$\zeta_{Sp} = f(Re_{Sp}, h_V) = \frac{A}{Re_{Sp}} \cdot H + C \cdot H \quad (24)$$

$$H = B \cdot \left(\frac{DN}{h_V}\right)^D + 1 \quad (24a)$$

For example, for a plate valve with narrow seat, let the constants assume the following values: A = 107; B = 74; C = 1.4; D = -2.4; DN is the inner diameter of the valve.
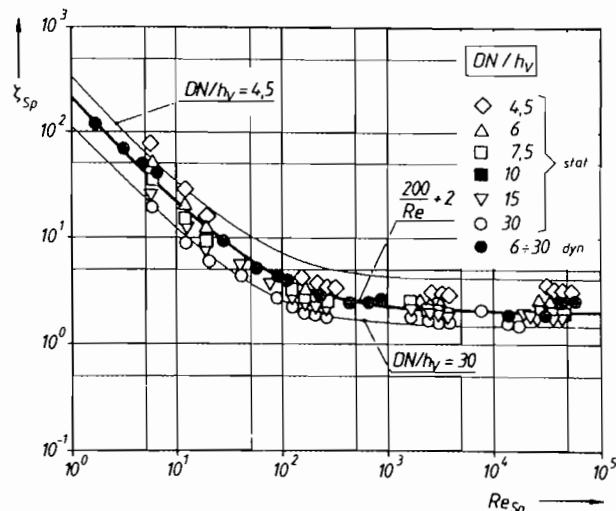

Figure 8. Resistance Coefficient ζ as Function of the Reynolds Number; Cone Valve with Narrow Seat 32mm ND.

As previously shown for the valve with narrow seat in Figure 7, the magnitude of the movement of the valve body becomes of diminishing influence when different opening widths result in increasingly similar flow patterns (Figure 9), as is the case with cone valves with broad seats.
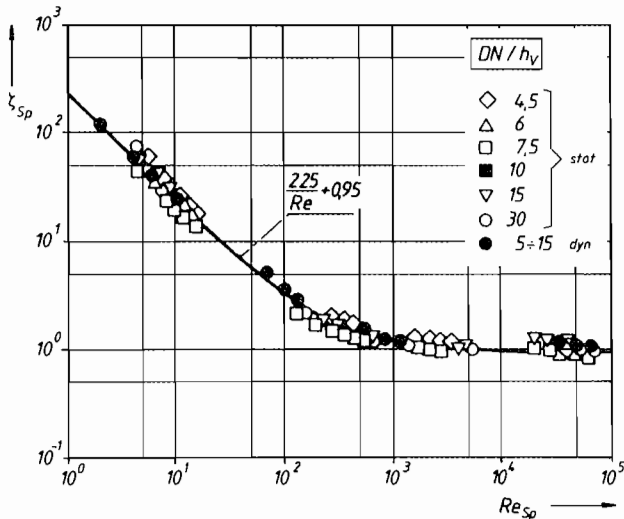

Figure 9. Resistance Coefficient ζ as Function of the Reynolds Number; Cone Valve with Wide Seat 30mm ND.

The coefficient of force Ψ, which is related to the coefficient of resistance ζ, as shown in Equations (10) and (21), also depends on Re_{Sp} and h_V.

Plotting static and dynamic tests for a plate valve (Figure 6 (a)) results in a scattering with a mean value Ψ = 0.5 (Figure 10). For a broader range of movement of the valve body, the dependency on the magnitude of this movement has to be taken into account.

In streamlined valve constructions, the coefficient of force Ψ decreases with the Reynolds number and with the opening relation DN/h_V (Figure 11). An approximate solution is given in

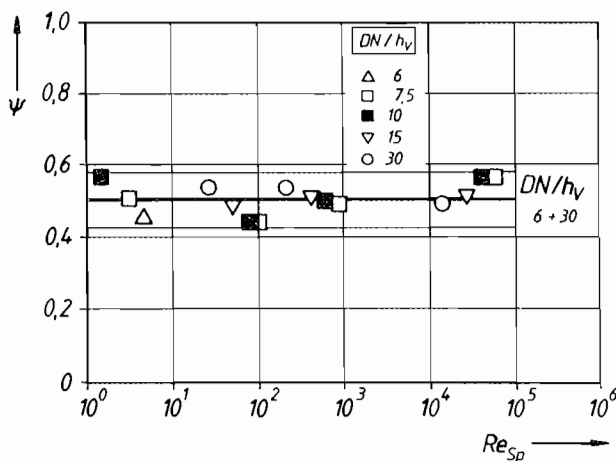$$\psi = K_1 - K_2 \cdot \log(Re) \qquad (25)$$

Figure 10. Force Coefficient Ψ as Function of the Reynolds Number, Plate Valve with Narrrow Seat 32mm ND, Spring Load p_o = 0.6 bar.
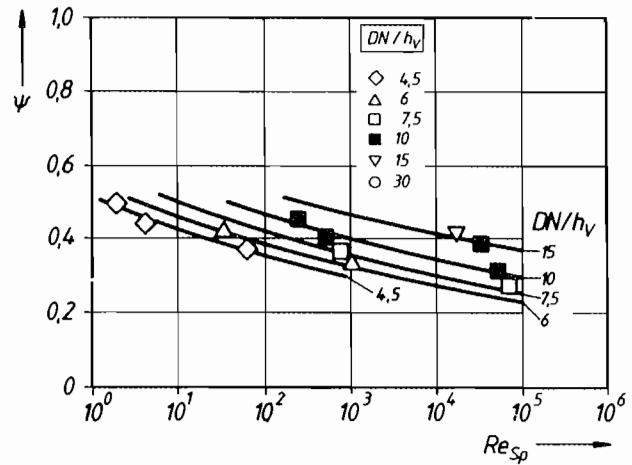

Figure 11. Force Coefficient Ψ as Function of the Reynolds Number, Cone Valve with Wide Seat 30 mm ND, Spring Load p_o = 0.4 bar.

(K_1, K_2 constants of the Ψ-Re-function). For the cone valve with small seat, for example (Figure 6 (b)), K_1 = (0.5-1.6) h_V/DN and K_2 = 0.075.

Currently, reliable stored empirical values for ζ and Ψ for certain valve types are the basis for the mathematical determination of kinematics and of pressure loss. Their stationary determination is as a rule, satisfactory. It is recommended to obtain data for certain valve types empirically in several test series.

MATHEMATICAL PREDICTION OF VALVE KINEMATICS AND PRESSURE LOSS

Computer based modelling, taking into account Reynolds number dependent equations for resistance and force coefficients ζ and Ψ, permits the exact prediction of the valve kinematics (Figures 12 and 13, a small portion of the comprehensive verification program). This is also valid for cone valves with broad seat and guide. The opening angle φ_O is entered in all calculations. The extreme case of pulsating displacement (for example, with high discharge pressure and consequently reduced efficiency) with shockwise phase rise of velocity was experimentally simulated using an additional device at the pump's working chamber with flying pneumatically loaded piston [9]. Here also, the computer model showed satisfactory results (Figure 14). Because of the simplification used, the numerical representation of the opening process can still be improved.

Other results indicate, however, that the customary values of the volumetric efficiency (η_V > 0.8) and the resulting starting phase section allow reliable calculation of the essential data, such as the maximum movement of the valve body, closing angle and pressure loss with maximum fluid displacement (Figure 15). The calculation requires as accurate values for ζ and Ψ as possible. If these values are taken from dynamic experiments, then the agreement between calculation and measurement is nearly perfect.

Using a simple approximation of measured values will necessarily lead to errors. It became evident that the relative deviation of the computation for valve lift, pressure loss and closing angles was always less than the plotted scattering of the empirical figures for ζ and Ψ. Experience in the selection of empirical sizes is necessary for a certain type of valve. It should be attempted to obtain calculated results for the pressure loss and closing delay that will result in safe operation.

The limits of the calculation become evident in Figures 15 and 16. In case of area contact (valve seat or limit) an additional adhe-
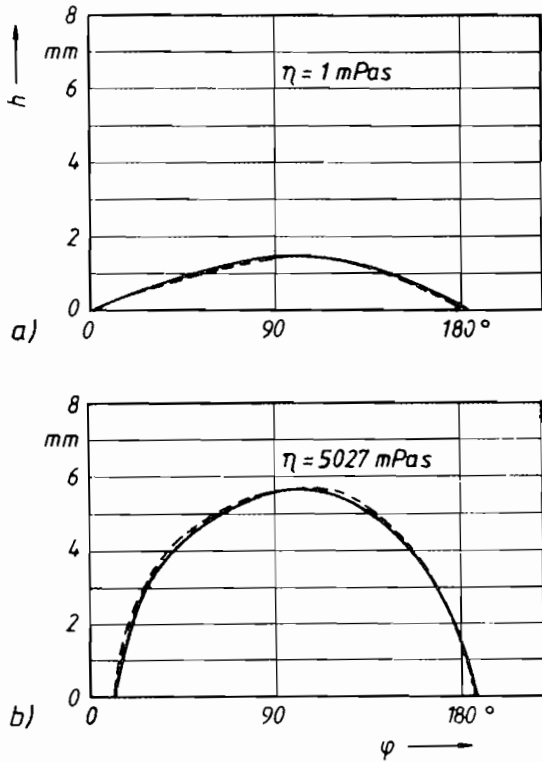
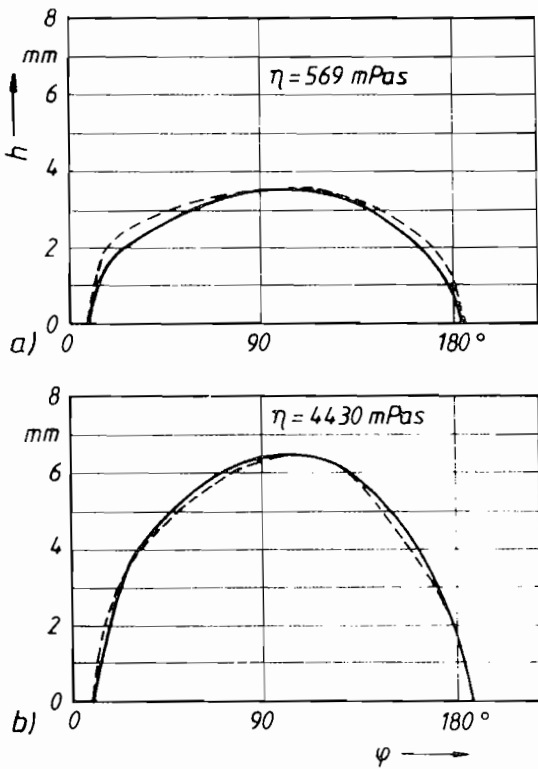Figure 12. Valve Kinematics. Plate Valve 32mm ND, Spring p_O = 0.6 bar, n = 200 min^{-1}. _ _ _ _ Measured, _____ Calculated.

Figure 13. Valve Kinematics. Cone Valve with Narrow Seat 32mm ND, Spring Load p_O = 0.6 bar: a) 200 min^{-1}, b) 100 min^{-1}. _ _ _ _ Measured, _____ Calculated.
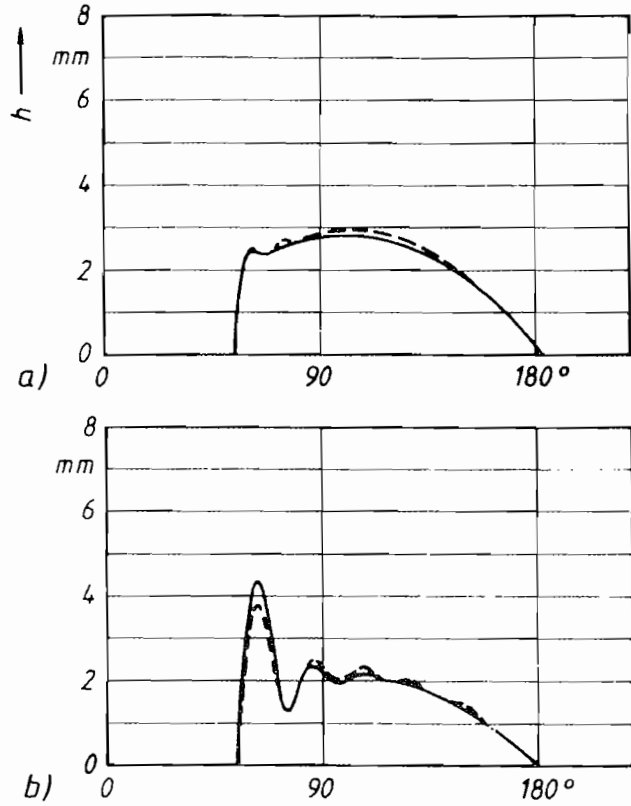

Figure 14. Valve Kinematics at Strong Phase Rise of Velocity a) Plate Valve 32 mm ND, Spring Load p_O = 0.1 bar, n = 200 min^{-1}, η = 1 mPas; b) Cone Valve 32 mm ND, Spring Load p_O = 0.1 bar, n = 200 min^{-1}, η = 1mPas; _ _ _ _ Measured, _____ Calculated.

sion force has to be overcome, which has not yet been really included in the present model.

The effect of the opening peak in Figure 15 can be of importance for the pressure determination. However, as far as cavitation is concerned, these peaks will hardly be significant. They are of short duration and will, in most cases, decay through formation of minute gas bubbles.

The adhesion of the valve body on its seat or cage (Figure 16) causes a significantly increased closing delay $\Delta\varphi_s$, which should always be considered in valve assembly design by keeping contact surfaces small or by using a contact-free working mechanism.

APPLICATION

With computer simulation, types of valves with known empirical resistance characteristics can be optimally designed — spring characteristics, valve mass, pressure loss, closing delay and closing energy. The reduction of the closing delay and closing energy by an increase of the spring load is schematically shown in Figure 17. Reducing the closing velocity by a factor of three will reduce the closing energy, simultaneously halving the valve mass by a factor of 20!

The pressure loss Δp determines the important NPSH$_r$ of a pump

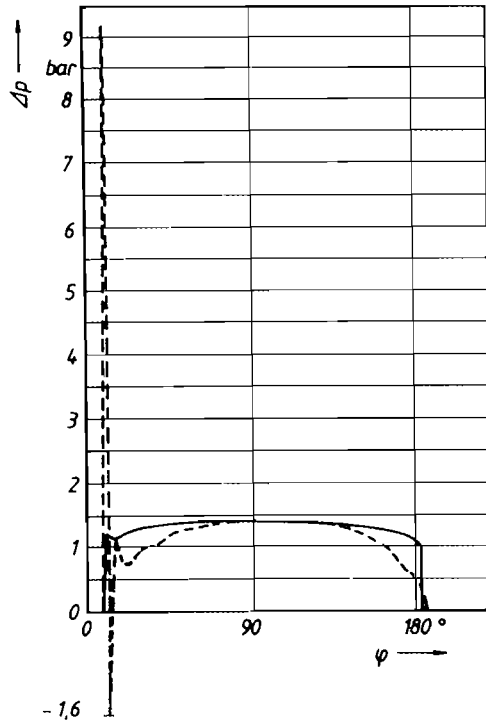$$NPSH_r = \frac{\Delta p}{\rho \cdot g} \qquad (26)$$

Figure 16. Valve Kinematics with Adhesion Effects, Cone Valve with Small Seat 32 mm ND, Spring Load p_{δ} = 0.1 bar, n = 200 min^{-1}, η = 600 mPas; _ _ _ _ Measured, ____ Calculated.

Figure 15. Pressure Loss Measured/Calculated, Cone Valve with Narrow Seat 32 mm ND, Spring Load p_O = 0.7 bar, n = 200 min^{-1}, η = 569 mPas; _ _ _ _ Measured, ____ Calculated.

Figure 17. Reduction of Closing Delay and Closing Energy. 1) weak spring 2) strong spring.

whereby (Figure 18) pressure variation in the suction line as well as pressure peaks caused by adhesion effects during valve opening will usually decay in the form of barely visible vapor bubbles. Stable pressure peaks (Figure 15) are only formed if the pressure level greatly exceeds the vapor pressure of the fluid.

A reduction of the NPSH$_r$ can be effected by the reduction of the fluid flow velocity (rpm of pump), spring loading, coefficient of resistance (for example, more streamlined flow geometry), as well as through an increase of the effective interior valve diameter (for example, double-flow plate valve).

WEAR

The intermittent valve operation (Figure 2) causes a stress on the material of the closing surfaces. The shocklike closing energy, as well as the intermittent (swelling) pressure on the closing surfaces, are exerting a stress on the material of construction through elastic and partially plastic deformation.

Together with the fluid, the following wear mechanisms are exerted in the operation of the pump:

• Material fatigue (increasing)

• Corrosion, respectively permanent removal of passivated layer

• Abrasion through solid particles (tribologic system of three materials)

Under certain operational conditions, *cavitational wear* (imploding vapor bubbles) can also play a part. Many ductile materials tend to harden (cold) and become more wear resistant through the hammer-like valve operation. Based on experience, it is possible to counteract the wear mechanisms a) and b) by selecting suitable valve construction and kinematic, as well as by a proper selection of construction materials (proper guidance of the valve body, limited closing energy, tenacious hard mate-
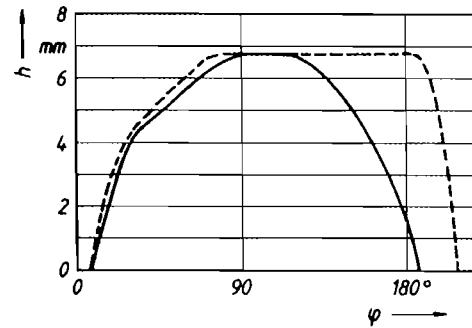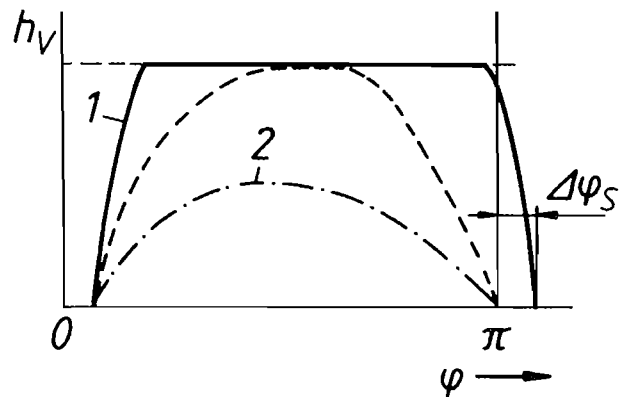
rials of high corrosion resistance, cone-shaped valve form).

Though basic research should further develop the empirical knowledge in this area of valve wear, most newer research has been performed on abrasive valve wear [10, 11, 12].

Experience shows that for higher pressure the separation of closure and support function is of advantage (Figure 19). The underlying thought is that wear particles should be pressed with the minimum of compression into the elastic sealing material and not damage it, whereby the sealing effect is fully maintained (Figure 14 (c)). Obviously, it is necessary to coordinate particle volume, solids content, elastomeric qualities and sealing volume.

Many types of valves with seal inserts (for example, Figure 6 (c)) are well suited for maximum particle diameters of 0.5 to 1.0 mm if the nominal width of the valve is not too small. Depending on the solids content or pressure, even larger particles can be handled.

Valves for oscillating displacement pumps, handling decidedly coarse slurries, have to be selected according to a different strategy (i.e, forced control of valves).

For low pressures elastomeric valve seats or balls are commonly used; however, it is then necessary to select a wider seating surface, and to reinforce balls by a core and the possible use of supporting stops (Figure 19 (a)).

For many suspensions it is not possible to find chemically and thermally resistant elastomers so that hard, mostly metallic seals, have to be selected (for example, catalyst suspensions). As a rule these suspensions contain very small particles (maximum
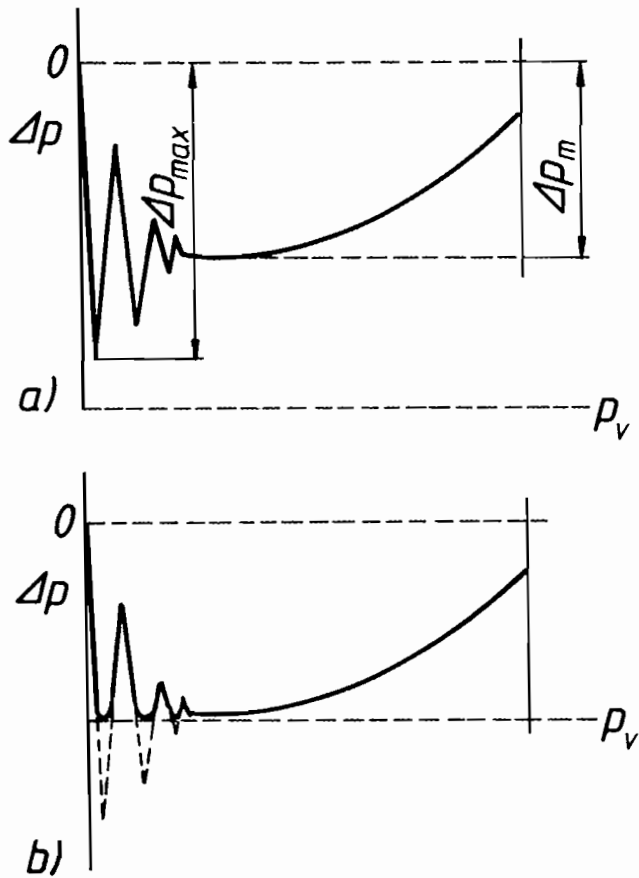
Figure 18. *NPSH$_r$ and Pressure Vibrations. p$_v$ vapor pressure.*

Figure 19. Sealing Bevel in Automatic Pump Check Valves. a) elastic, b) rigid, c) supporting seal, d) supporting seal (detail).

particle size 200 µm). In case of hard sealing surfaces, both sealing and support functions coincide (Figure 19 (b)). Based on experience, small contaminations of abrasive particles increase the wear enormously.

TRIBOLOGICAL SYSTEM

In the closing positions (Figure 20, right II-IV), which is most responsible for the wear, particles are clamped under high com-

pression when the differential pressure (in pumping chamber p$_A$) presses onto the valve body and the pressure (compression) on the sealing surfaces p̄ is high. The (partially broken) clamped particles establish a miniature clearance through which fluid can stream back under the differential pressure (III). Single particles of approximately the size of aperture furrow along the aperture wall removing "shavings" (IV).
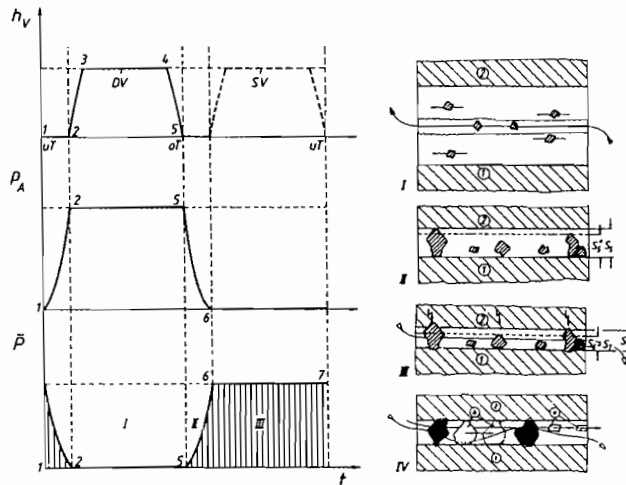

Figure 20. Schematic View of Valve Operation as Function of time t, hv lift of valve body, pA pumping chamber, p̄ pressing of seal I valve open, II valve closes, III valve closed, IV back flow wear 1 valve seat, 2 valve body, oT upper, uT lower dead point of plunger, t time. a) small particle flows with fluid, b) large particle clamped.
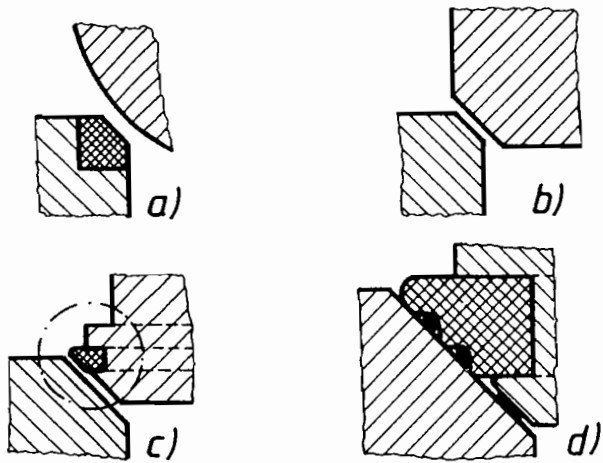
WEAR CHARACTERISTIC IN FIELD SERVICE

In the field, the wear rate usually increases with an increase of the differential pressure and stroke frequency (Figure 21). With increasing stroke frequency a lesser increase of wear can be observed due to a shorter time of engagement. The lesser increase with the differential pressure probably becomes less as more particles fracture.

While the rate of wear below the relative hardness $H_p/H_W < 0.9 - 1.0$ is nearly constant in time and place, the tribosystem tends to be unstable beyond this range. This becomes evident in easily reproducible sudden valve failure through radial erosion (radial grooves, "worm holes") (Figure 22). This instability is obviously dominated by the relative hardness; however, valve geometry and valve material are also factors.

• A cone-shaped sealing area appears more desirable than a flat one.

• A wear part that easily rotates when in use is markedly more resistant to radial erosion, as initial grooves tend to even out into wear areas. The experience with free-moving ball valves confirms this.

• Heterogeneous hard materials, for example, stellite with tungsten carbide enclosures, show higher wear resistance also against radial grooves, which can be easily imagined (Figure 21 (b)).

The closing energy though has lesser importance for lighter valve body and greater significance for heavier balls. Of interest is (Figure 21 (a) and (d)), Ap = 2 bar) the progressive increase of wear with the stroke frequency, as shown in Equation (3).

Field tests which were performed (Figure 23) with different materials [10, 11, 12] also showed minor influences of valve

geometry (cone, ball plate), which will not be discussed here.

The rate of wear usually increases with the relative hardness H_p/H_w; whereby the degree of rise near $H_p/H_w = 1.0$ is too steep (Figure 24). This fact is also known from other tribological systems. In some material combinations, even homogenous fluids (without abrasive particles) show minimal wear rates.

More pronounced are the influences of solids concentration and particle size (Figures 25 and 26). The width of the sealing surface plays a minor roll, unless it is less than 20-30 times the mean particle size diameter.
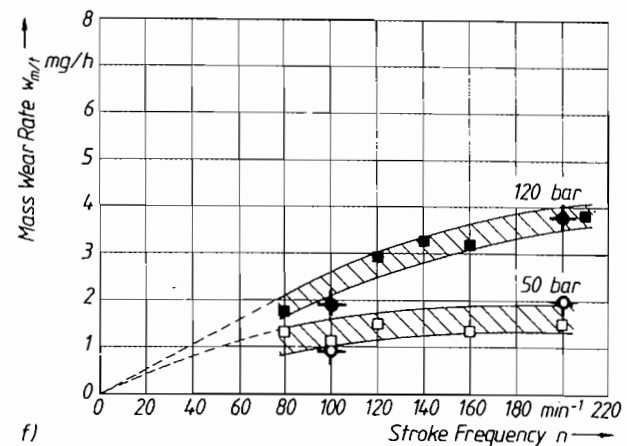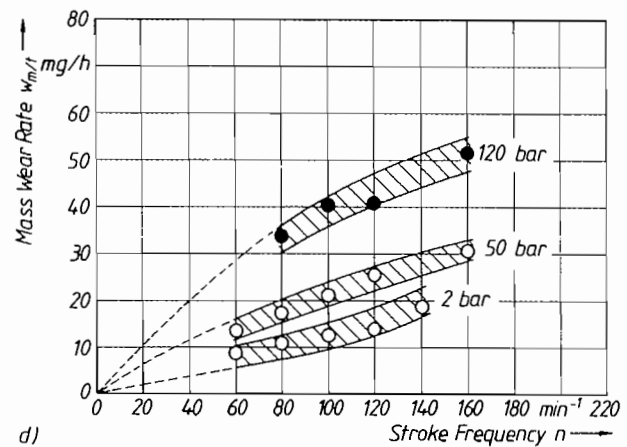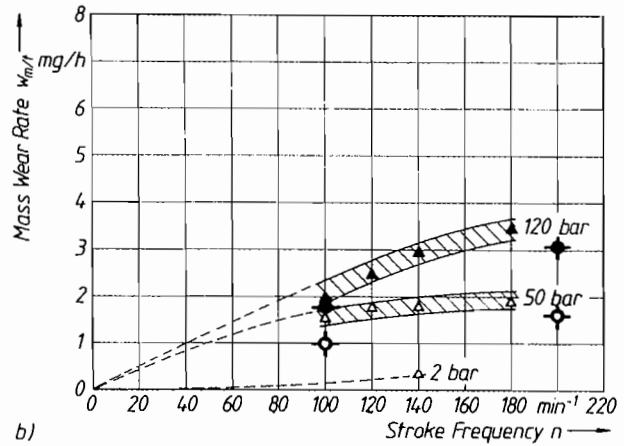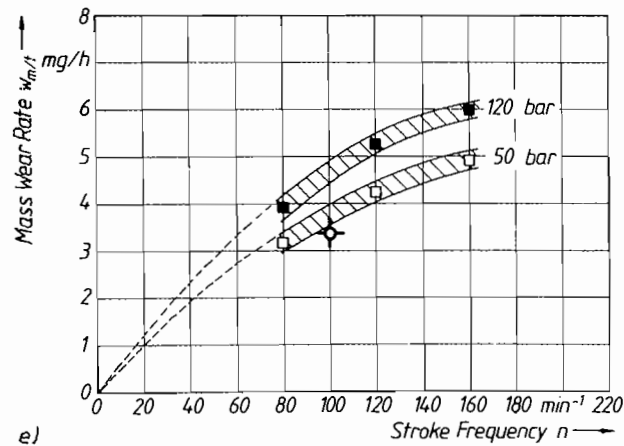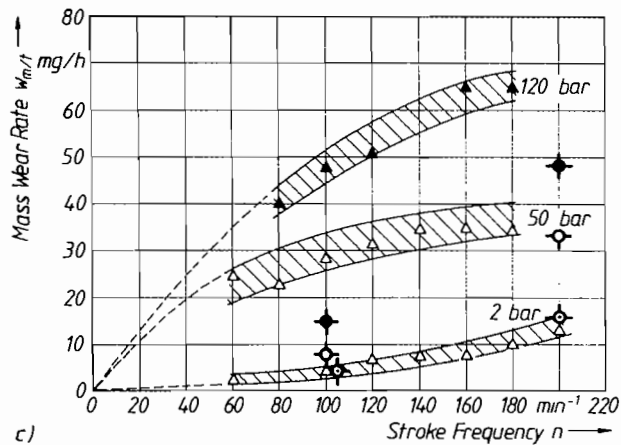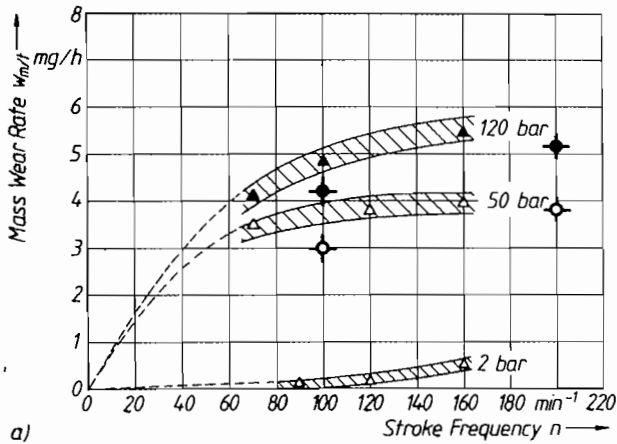

Figure 21. Mass Wear Rate of Different Pump Check Valves. a) cone, Cr-Steel L.4528/10 percent feldspar in water suspension. b) cone, Stellite 10 percent feldspar in water suspension. c) cone, hardmetall GT30/ 15 percent quartz in water suspension. d) ball, hardmetall GT30/ 15 percent quartz in water suspension. e) plate, hardmetall GT30/ 10 percent feldspar in water suspension. f) plate, hardmetal GTC/ 10 percent feldspar in water suspension.
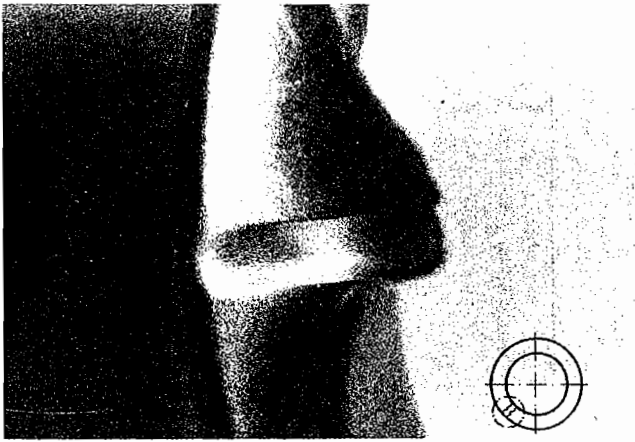
Figure 22. Radial Erosion of Cone Valve (Cr-Steel 1.4528 after 4 h ten percent quartz sand in water suspension, n = 100 min⁻¹, p = 120 bar).
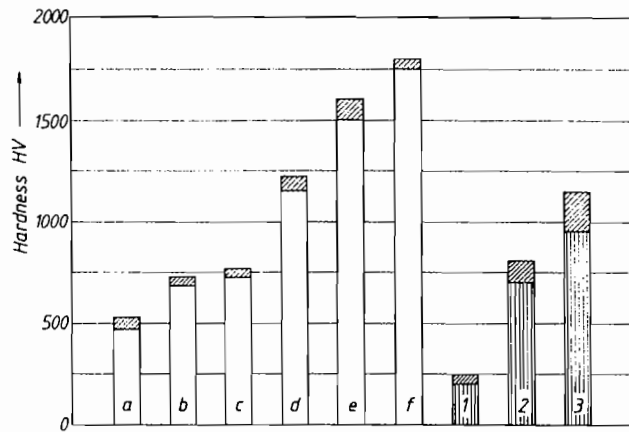

Figure 23. Valve Materials and Solid Particles. a) Cr-steel 1.4034, b) Cr-steel 1.4528, c) stellite 20, d) hardmetal GT30, e) hardmetal GTC, f) silicon nitride. 1) limestone, 2) feldspar, 3) quartz.

Tribometric Simulation

In most practical applications, particle mixes of unknown hardness are encountered. This requires a tribometric wear prognosis that should be performed with close to actual valve geometry and working conditions. The tamping tribometer (Figure 27) permits the simulation of the compressing of the closing surfaces of the check valves with real suspensions without flow pressure; consequently, it is easy to operate. The suspension is circulated without pressure through the apparatus that contains the wear parts (Position 2, 3) under steady pounding.

Field test and tribometric tests (Figure 21, points with cross) coincide for all practical purposes (Figure 21 (a), (b), (e), (g)) if the tribosystem is operated in its stable range (Hp/Hw < 0,9). In the range of high wear Hp/Hw ≈ 1.0 (Figure 21 (c)), larger deviations occur, and it is advisable to multiply the wear rates obtained in the tribometer by a safety factor of 1.5 to 2.0. Wear rates for the prognosis of durability obtained in tamping tribometer experiments contain all the influences of valve geometry, material of construction, particle size, solid concentration, etc. The conversion to other dimensions can be easily achieved.
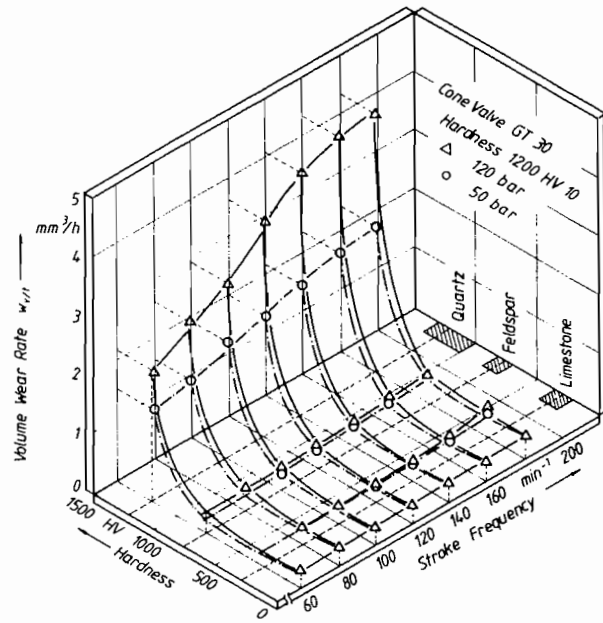

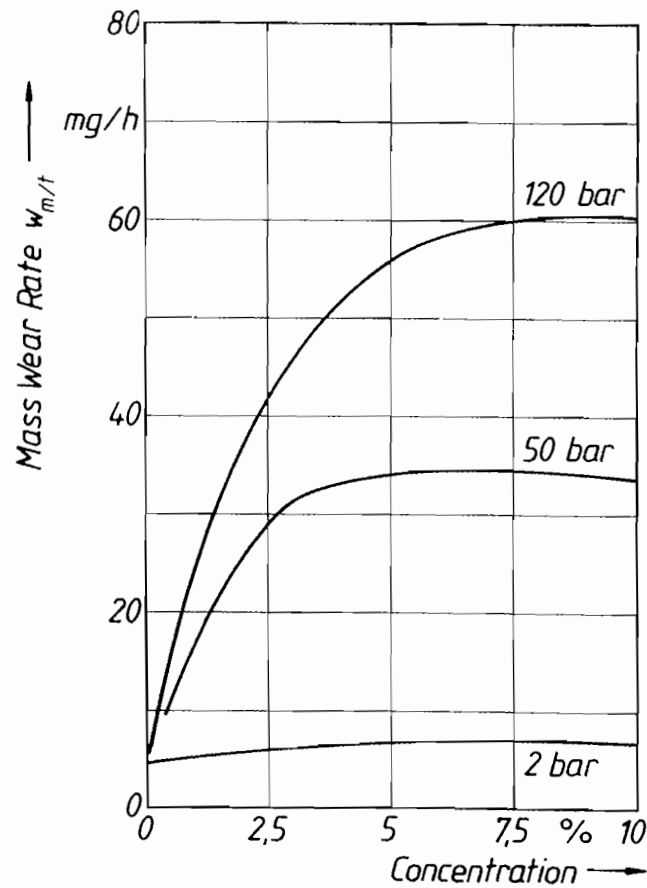Figure 24. Wear Characteristics of a Cone Valve (Hardmetal GT30).

Figure 25. Influence of Solids Concentration (120 bar, 160 min⁻¹). Cone valve, hardmetal GT 30, ten percent quartz in water suspension.
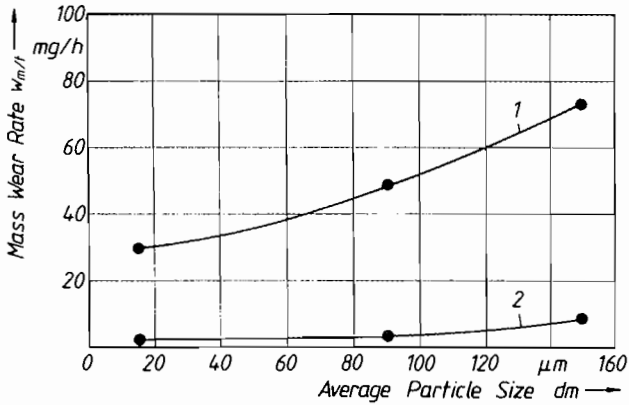
Figure 26. Influence of Particle Size (120 bar, 160 min⁻¹). 1) Cone valve, hardmetal GT 30, ten percent quartz in water suspension, 2) Cone valve, hardmetal GTC, ten percent quartz in water suspension.
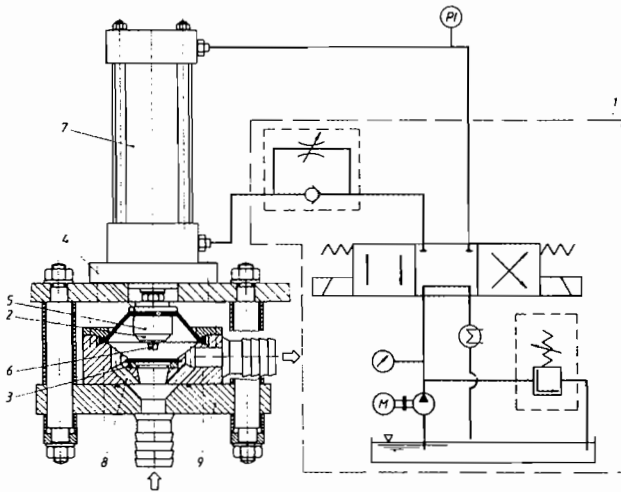

Figure 27. Tamping Tribometer. 1) hydraulic system, 2, 3) wear parts (cone, seat), 4, 5, 6, 7) actuating parts, 8, 9) attachment parts.

The suitability of the tamping tribometer for the simulation of a real tribosystem means (and this is the only real difference) that the radial erosion is of minor significance, which is the case in the stable range.

Nevertheless, information relating to the stable range are required for suspensions of unknown hardness characteristics. Usually an estimate can be made due to the chemical composition of the solids, such as Al_2O_3, SiO_2, limestone, feldspar, etc. Beyond this, tests with Miller's sliding tribometer [12] indicate that a connection exists between Miller's number (MZ) and Vicker's hardness (HV) (Figure 28), though this connection also depends on the particle size. However, the "representative hardness" of a specific wear material can be determined, and with it the limit of stability can be estimated according to the criteria Hp/Hw < 0.9.

Different test series also indicated that the Tribosystem is stable only if the SAR number (SAR = MZ × ρw/ρp) is below 90-100. This is valid for fine abrasive particles below a mean particle size of 100 μm. The SAR number is a most valuable piece of information for the wear characteristic of a construction material, as shown by the comparison of the following data:
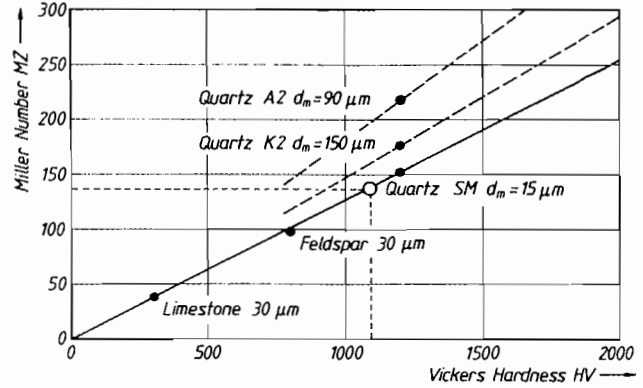
Figure 28. Miller Number and Vickers Hardness of Solids.

a) Stellite 20/Feldspar (d_m — 30μm)   SAR-69
b) Chromium alloy 1.4528/Feldspar (d_m — 30μm)   SAR-103

Actually, extensive field tests indicate that the tribosystem a) is in the stable range, while b) is not, though the relative hardnesses differ only slightly (Figure 29).

DESIGN STRATEGY

Based on field tests and tribometric examinations, the design strategy as shown in (Figure 29) can be deduced for the automatic check valves with metallic seal surfaces. If for a given suspension a primary valve selection (geometry, material of con-

Figure 29. Design Strategy for Pump Check Valves.

struction) has been made, then Miller's tribometer can give an indication as to the stability via the SAR number. For a stable condition, the specific volume wear rate (For example, W_{VNSHt} mm^3/mm^{2}h) can be established with the tamping tribometer, which predicts the life expectancy L_h (Figure 28), taking into account the available wear volume (Design size $\bar{V}$).

The life expectancy can be optimized by repeated application of this selection process with different materials of construction.
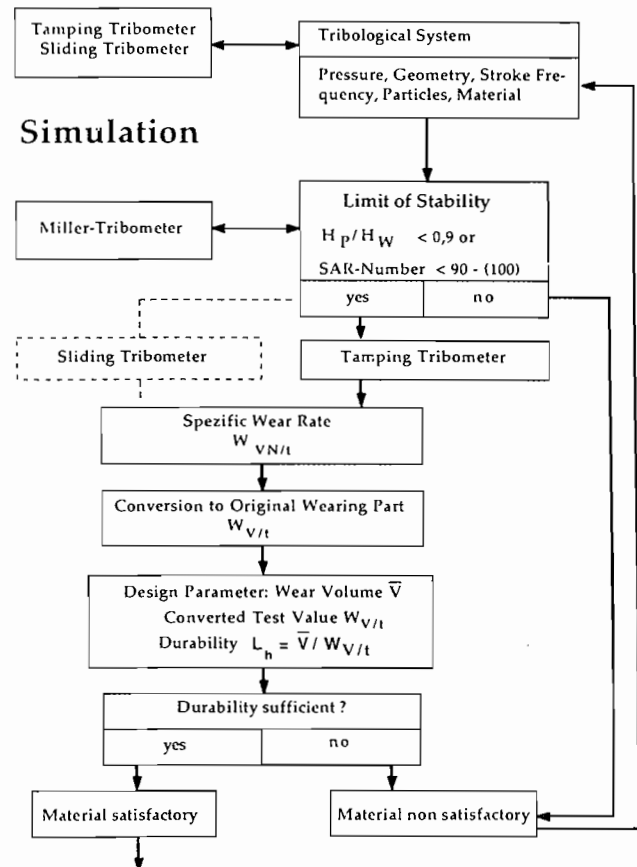
If the tribosystem is inherently unstable, and if a suitable material of construction cannot be found, the only remaining solution is the selecting of a construction with a supporting seal (Figure 6(c)). The excessive increase of hardness, possibly by the use of hard and brittle sintered ceramic materials (Silicon nitride, etc.), is frequently not successful due to the danger of fracture and disintegration.

CONCLUSIONS

The method introduced for the computation and for optimizing of the working mechanism of automatic check valves for pumps permits a precise prediction of the volumetric efficiency and NPSH$_r$ for Newtonian fluids.

The most suitable valve design can be easily found for a type of check valve if its resistance performance is known. In the future some additional improvements of the calculation process will be attempted by the inclusion of the influences of adhesion and friction. The broadening of the calculation method to include non-Newtonian fluids that follow the power law will also be attempted.

Scrutiny of valve wear, using abrasive suspensions, led for the first time to a prognosis of durability. In addition to much detailed knowledge of the behavior of the specific tribosystems of automatic check valves, it is important that a realistic simulation is performed on the discussed tramping tribometer.

If the criterion of stability is observed (SAR 90–100), then the design strategy will lead to safe check valves with a calculable durability.

As the criterion of stability depends on the particle size, it is also desirable to examine this influence in the future. Furthermore, the influence of the rheology of fluids on wear and stability should also be investigated.

NOMENCLATURE

Symbol	Unit	Description
A,B,C,D	—	constants of the ζ-Re-function
A_K	m^2	cross section of the piston
A_{sp}	m^2	aperture area for plate valves
A_V	m^2	cross section of the valve body
A_{VF}	m^2	valve seat area
DN	m^2	nominal diameter of the check valve (seat opening)
d_h	m	hydraulic diameter of aperture
d_K	m	diameter of the piston
d_V	m	outer diameter of the valve body
d_{Vm}	m	mean diameter of the seat
E_s		specific closing energy
F	N	force
F_{Ad}	N	force of adhesion
F_a	N	force of inertia
F_D	N	force of damping
F_F	N	force of spring
F_{FO}	N	spring tension
F_G	N	weight force
F_N	N	normal force
F_R	N	force of mechanical friction
F_{St}	N	force of the fluid stream
F_V	N	force of displacement
g	m/s^2	gravitational acceleration
H		constant
H_p, H_w		hardness (particle, material)
h_K, h_{Kmax}	m	stroke length of plunger, maximum stroke length
h_V, h_{Vmax}	m	movement of valve body
$\dot{h}_V$	m/s	velocity of the valve body
$\ddot{h}_V$	m/s^2	acceleration of the valve body
K_1, K_2	—	constants in the ψ-Re-function
k_F	N/m	spring constant
L_h	h	durability
l	m	length of the connecting rod
l_{Sp}	m	length of aperture
m	kg	mass of the valve body
m_F, m_V	kg	mass of the valve spring and body
n	min^{-1}	speed
p	bar	pressure
Δp	bar	pressure differential
p_o	bar	s. text and figures
p_u	bar	s. text and figures
p_o^*, p_u^*	bar	s. text and figures
p_O	bar	opening pressure of a spring-loaded check valve
Re, Re$_{Sp}$	—	Reynolds Number (at clearance: Sp)
r	m	radius
r_V	m	radius of the valve body
r_K	m	crank radius
$\dot{V}_{MAT}$		volume of valve body
$\dot{V}_{dp}$		elasticity volume
$\dot{V}_{Sp}$		flow volume through the valve aperture
v_K	m/s	plunger velocity
Δv_K	m/s	velocity jump
v_{sp}	m/s	fluid velocity through valve aperture
W_{Vt}	mm^3/h	wear rate (volume)
$W_{VN/t}$	$_{mm}$^{3}/mm^{2}h	specific wear rate (volume)
W_{VNSHt}	mm^3/mm^{2}h	specific wear rate (volume) from tribometer
α	deg	angle of the valve closure area to the center axis of the valve
ε		coefficient
ζ		resistance coefficient
ζ_{Sp}	—	resistance coefficient relating to clearance
η	pas	dynamic fluid viscosity
η_E	—	elasticity factor
η_G	—	quality (slip) factor
$\Delta\eta_{Gl}$		degree of quality loss
$\Delta\eta_{GS}$		degree of quality loss
$\Delta\eta_{GSd}$		degree of quality loss
$\Delta\eta_{GSs}$		degree of quality loss
η_v	—	volumetric efficiency
ϑ	Ns/m	damping factor

λ_K	—	connecting rod relation
μ		friction coefficient
ρ, ρ_{Fl}	kg/m^3	density, fluid density
ρ_{Mat}	kg/m^3	density of the valve body
φ	deg	crank angle
$\varphi_{Ö}$	deg	opening angle of check valve
φ_S	deg	closing angle of check valve
$\Delta\varphi_S$	deg	closing delay
ψ	—	force coefficient
ω	s^{-1}	angular velocity
U.T.		lower dead point
O.T.		upper dead point
NPSH$_r$		net positive suction head required
MZ		Miller Number
HV		Vickers Hardness
SAR		SAR Number
DS		discharge stroke
SS		suction stroke
DV		discharge valve
SV		suction valve

REFERENCES

1. Vetter, G., Ausführungskriterien und Störeinflüsse bei oszillierenden Dosierpumpen; in Jahrbuch Pumpen (Hrsg.: G. Vetter), Vulkan-Verlag, Essen, pp. 521-529 (1987).

2. Vetter, G., and Störk, U., Verschleiss selbsttätiger Pumpenventile durch abrasive Suspensionen; Chem.-Ing.-Tech. 59 No. (5), pp. 383-392 (1987).

3. Adolph, U., Vorausberechnung der Funktion und der Schlaggrenze selbsttätiger Flachsitzventile von Kolbenpumpen bei reiner Flüssigkeitsströmung; Dissertation TU Dresden (1967).

4. Hadlatsch, P., Berechnung der Druckwellen in Brennstoffeinspritzsystemen und in Hydraulischen Ventilsteuerungen; Forschungsbericht des Landes Nordrhein-Westfalen (1983), Westdeutscher Verlag Köln und Opladen (1961).

5. Vetter, G., Fritsch, H., and Müller, A., Einflüsse auf die Dosiergenauigkeit oszillierender Verdrängerpumpen, Aufbereitungs-Technik 15 (1), pp. 1-12 (1974).

6. Fritsch, H., and Jarosch, J. Einflussparameter auf die Genauigkeit Von Dosierpumpen, Chem.-Ing.-Tech. 58 No.(3), pp. 242-243 (1986).

7. Vetter, G., and Thiel, E. "Kinematics of Automatic-Pump Valves of Reciprocating Positive Displacement Pumps Discharging Newtonian Fluids, Lecture Pump Congress Karlsruhe, preprint Section C4 (1988).

8. Vetter, G., and Fritsch, H., Untersuchungen zur Kavitation bei oszillierenden Verdrängerpumpen, Chem.-Ing. Technik, pp. 271-278 (1969).

9. Vetter, G., and Schweinfurter, F. Druckschwingungen durch oszillierende Verdrängerpumpen in Rohrleitungen, VDI-Bericht 603, pp. 293-318 (1986).

10. Störk, U., and Vetter, G. "Wear of Check Valves of Reciprocating Displacement Pumps Caused by Abrasive Suspensions," Pump Congress Karlsruhe reprint Section C8 (1988).

11. Störk, U., Verschleiss selbständiger Pumpenventile oszillierender Verdrängerpumpen mit abrasiven Suspensionen, Dissertation Universität Erlangen (1988).

12. ASMT G 2.3, Standard Test Method for Slurry Abrasivity (Miller-Number) Determination 11-16-80 (1980).